Chapter 3

Neutral Gas

3.1 Absorption lines

Absorption coefficient

$$\varkappa_\nu = \frac{c^2 \cdot n_l \cdot g_u}{8\pi \cdot \nu^2 \cdot g_l} \cdot A_{ul} \cdot \left[1 - \exp\left(-\frac{h\nu_0}{k_B \cdot T_{\text{ex}}}\right)\right] \cdot \phi_{ul}(\nu) \tag{3.1}$$

n_l	=	number density of particles in lower state
g_u	=	statistical weight of upper state
g_l	=	statistical weight of lower state
A_{ul}	=	probability for spontaneous emission
ν_0	=	emission frequency
T_{ex}	=	excitation temperature
$\phi_{ul}(\nu)$	=	normalized spectral distribution ("profile shape")

Interstellar absorption lines much narrower than stellar ones.

Visible, UV, NIR: atoms (Na, K, Ca), ions (Ca^+, Ti^+), molecules (CN, CH, CH^+, C_2, OH)

FUV: Lyman series of H; molecules, in particular H_2 (HST, FUSE)

Radio: HI, OH against strong (mostly synchrotron) continuum sources

In what follows we work out how one can determine column densities from absorption lines. Equivalent width of a line defined by

$$W = \int_0^\infty \frac{I_C - I_\lambda}{I_C} d\lambda \tag{3.2}$$

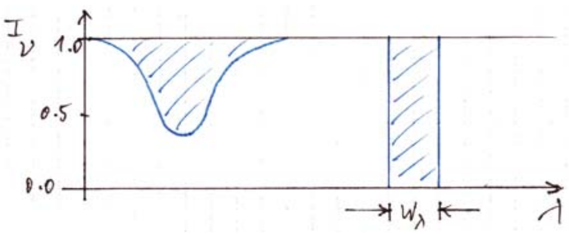

Figure 3.1: Definition of the equivalent width

where I_C is the intensity of the stellar continuum on either side of the line; given in units of wavelength. With only absorption radiative transfer reads

$$I_\lambda = I_{0,\lambda} \cdot e^{-\tau_\lambda} \tag{3.3}$$

where

$$\tau_\nu = \int_0^{s_0} \varkappa_\nu ds \tag{3.4}$$

is the optical depth. Hence

$$W_\lambda = \int (1 - e^{-\tau_\nu}) d\lambda = \int (1 - e^{-\tau_\nu}) \frac{d\nu}{c} \cdot \lambda \tag{3.5}$$

For small optical depth

$$W_\lambda = \int \tau_\nu d\lambda = \int \tau_\nu \lambda^2 \frac{d\nu}{c} \tag{3.6}$$

Let us assume that $h\nu \ll k_B T_{\rm ex}$ (always valid in FIR and higher frequency regimes):

$$\varkappa_\nu = \frac{c^2 \cdot n_l \cdot g_u}{8\pi \cdot \nu^2 \cdot g_l} \cdot A_{ul} \cdot \phi_{ul}(\nu) \tag{3.7}$$

Integration over the line-of-sight will convert number density n_l into column density N_l

$$\varkappa_\nu = \frac{c^2 \cdot N_l \cdot g_u}{8\pi \cdot \nu^2 \cdot g_l} \cdot A_{ul} \cdot \phi_{ul}(\nu) \tag{3.8}$$

One often uses the oscillator strength

$$f = \frac{m_e \cdot c^3}{8\pi^2 \cdot e^2 \cdot \nu^2} \cdot A_{ul} \cdot \frac{g_u}{g_l} \quad \Rightarrow \quad \tau_\nu = \frac{\pi \cdot e^2 \cdot N_l}{m_e \cdot c} \cdot \phi_{ul}(\nu) \cdot f \tag{3.9}$$

so that

$$W_\lambda = \int_0^\infty \left[1 - \exp\left(-\frac{\pi e^2}{m_e c} \cdot N_l \cdot f \cdot \phi_{ul}(\nu)\right)\right] \lambda^2 \frac{d\nu}{c} \tag{3.10}$$

In all of the above it was assumed that various quantities do not vary along the line-of-sight.

3.1.1 Shape of line profile

Shape of line profile $\phi_{ul}(\nu)$ depends on intrinsic (natural) line profile and broadening effects (Doppler and pressure broadening). Natural line profile is given by the Lorentz curve

$$L(\nu) = \frac{1}{\pi} \cdot \frac{\gamma/2}{[2\pi(\nu - \nu_0)^2] + (\gamma/2)^2} \tag{3.11}$$

The lifetime τ of the transition is the reciprocal of the damping constant γ. The function is normalized such that

$$\int_0^\infty L(\nu) d\nu = 1 \tag{3.12}$$

Individual atoms move about according to the temperature of the gas. This gives rise to the so called Doppler profile ($\Delta\nu$ = Doppler shift, $\Delta\nu_D$ = Doppler width)

$$D(\nu) = \frac{1}{\sqrt{\pi}\Delta\nu_D} \cdot e^{-\left(\frac{\Delta\nu}{\Delta\nu_D}\right)^2} \tag{3.13}$$

which results form translating Maxwell-Boltzmann velocity distribution to frequency. Real line profile is the convolution of $L(\nu)$ and $D(\nu)$:

$$\phi(\nu) = \int_{-\infty}^{+\infty} L(\nu - \nu') \cdot D(\nu') d\nu' \tag{3.14}$$

the so called Voight profile. It requires to calculate the integral

$$\phi(\nu) = \frac{\alpha}{2 \cdot \pi^{5/2} \cdot \Delta\nu_D} \cdot \int_{-\infty}^{+\infty} \frac{e^{-y^2}}{(z-y)^2 + \alpha^2} dy \tag{3.15}$$

where

$$\alpha = \frac{\gamma/2}{2\pi \cdot \Delta\nu_D}, \qquad z = \frac{\nu - \nu_0}{\Delta\nu_D}, \qquad y = \frac{\Delta\nu}{\Delta\nu_D} \tag{3.16}$$

Common practice: Use of dimensionless equivalent width, i.e. (referred to centre frequency, wavelenght or velocity)

$$W = \frac{W_\lambda}{\lambda_0} = \frac{W_\nu}{\nu_0} = \frac{W_v}{c} \tag{3.17}$$

Now consider three cases concerning opacity:

1. optically thin case, $\tau \ll 1$, damping effects neglible

   $$\boxed{W = \frac{\pi e^2}{m_e c^2} \cdot N_l \cdot \lambda \cdot f} \tag{3.18}$$

   Measured equivalent width directly proportional to column density.

2. intermediate optical depth No analytic solution of integral for W_λ exists. Approximation yields

   $$W \propto \log(N_l \cdot \lambda \cdot f) \tag{3.19}$$

3. large optical depth, $\tau \gg 1$ In this case (Unsöld, 1955)

   $$W \propto \sqrt{N_l \cdot \lambda \cdot f} \tag{3.20}$$

   For still stronger lines absorption in the line wings becomes possible, hence the damping part of the line profile now dominates the "Doppler core".

$$\alpha \to 0 \Rightarrow \qquad H(\alpha, z) \to e^{-z^2} \qquad \text{doppler dominated} \tag{3.21}$$

$$\alpha \to \infty \Rightarrow \qquad H(\alpha, z) \to \frac{\alpha}{\sqrt{\pi}(z^2 + \alpha^2)} \qquad \text{broad damping wings} \tag{3.22}$$

$$\phi(\nu) = \frac{1}{\Delta\nu_D \cdot \sqrt{\pi}} \cdot H(\alpha, z) \tag{3.23}$$

$$H(\alpha, z) = \frac{\alpha}{\pi} \cdot \int_{-\infty}^{+\infty} \frac{e^{-y^2}}{(z-y)^2 + \alpha^2} dy \tag{3.24}$$

3.1.2 Curve of growth

At low optical depth, damping effects are small compared to Doppler broadening; shape of line profile is approximatly that of Doppler function. Equivalent width is proportional to column density; for intermediate column densities the equivalent width depends only litte on column density ⇒ "Doppler plateau"; for very large column densities, the equivalent width is governed by the damping-part of the line profile.

Example: curve of growth for different absorption lines (elements) observed towards the same cloud; if their Doppler boradening is the same, the growth curve is a single line up to the end of the Doppler plateau; they split in the damping regime, owing to different trasition probabilities, hence damping constants.

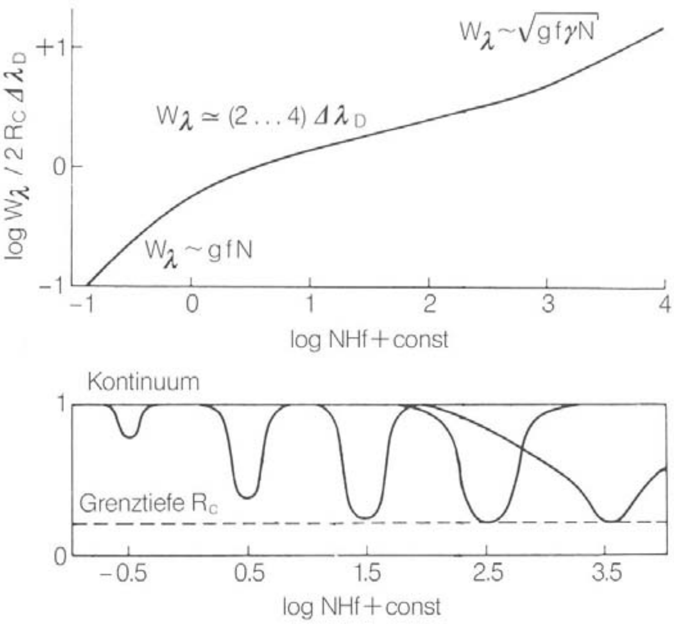

Figure 3.2: Curve of growth

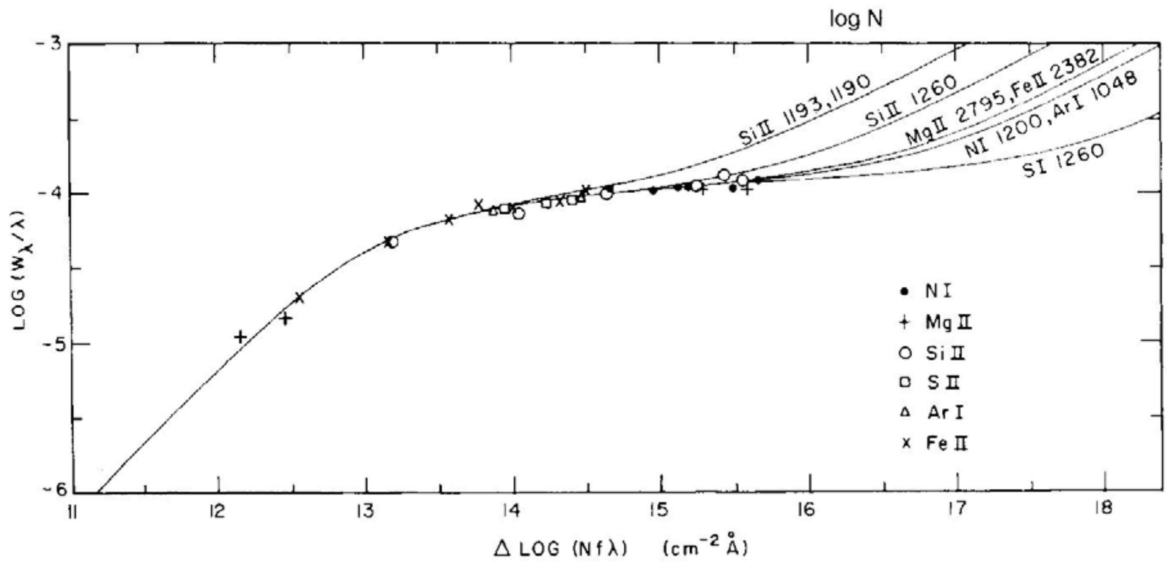

Figure 3.3: Observed curve of growth

In the general ISM it is the Doppler broadening that mostly dominates emission and absorption lines. Dampings wings are seen in stellar absorption spectra (collisional broadening). Outside of stars broad wings are seen in the absorption lines of “Damped Lyman α sysyems” (DLA).

ISM: most absorption lines lie in UV range

optical
- D_1 and D_2 doublet of neutral Na (5889 - 5895 Å) but always saturated $\rightarrow$ better use UV lines of Na at 3302.4 Åand 3303.0 Å
- H and K doublet of Ca^+ at 3933 Åand 3968 Å
- neutral Ca at 4226 Å

UV a host of lines, mostly saturated $\rightarrow$ column densities difficult to derive

Main goal: determination of abundances; referred to strong Ly α at 1215.67 Å; almost always damping in part of cog $\rightarrow$ column density can be derived.

Difficulty with other elemtents: column density can only be derived if all possible ionization states are measured; O and N and noble gases are not ionized in “neutral medium”

- one problem in determination of abundances: heavy elements may be depleted, owing to condensation onto dust grains.

- another method of abundance determination is to use emission lines from HII regions; these are close to solar, except for Fe, which is underabundant (most likely due to depletion onto dust grains)

- cosmological significance: dtermination of primeordial He abundance; we expect $Y = 0.25$ (by mass and 0.08 by number) abundance of N and O measured in low-metallicity galaxies (dwarf galaxies); measure Y as a function of N and/or O and extrapolate to zero N and/or O; the ordinate should then indicate primordial He abundance.

- results: $Y_{\rm gas} = 0.245 \pm 0.006$, $\quad Y_{\rm stars} = 0.232 \pm 0.009$, $\quad \langle Y \rangle_{\rm Prim.} = 0.239$, very close to prediction!

We shall encounter another cosmological application of absorption lines, viz. of molecules, in a cosmological context.

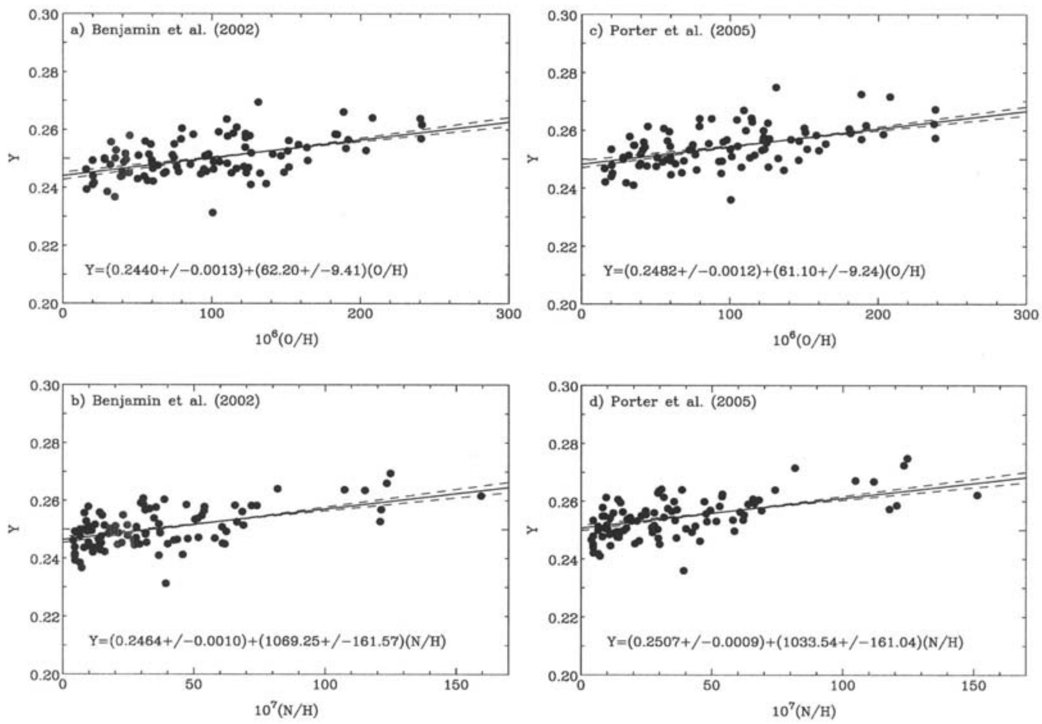

Figure 3.4: Determination of primordial abundance of H

3.2 Neutral atomic hydrogen

3.2.1 Transition

In the cold ISM, atomic hydrogen is neutral and in its ground state $1^2S_{1/2}$. Hyperfine splitting produces two energy levels of trhis ground state, owing to the interaction of the proton and electron spins. Description $n^{2S+1}L_J$

$S =$ total spin quantum number

$L =$ total orbital angular momentum quantum number

$J =$ total angular momentum (for the electrons) quatum number $= L + S$

$I =$ nuclear spin quantum number

$F =$ total angular momentum (for the atom) quantum number $= I + J$

$n =$ electronic quantum number

here: $n = 1, \quad S = 1/2, \quad L = 0, \quad I = 1/2, \quad J = 1/2 \Rightarrow F = 0, 1$

The probability for a spontaneous transition from the higher state $F = 1$ to the lower state $F = 0$ is extremely low:

$$A_{10} = 2.86888 \cdot 10^{-15} \quad \mathrm{s}^{-1} \qquad \text{magnetic dipole radiation} \tag{3.25}$$

i.e. this would occur once everey 11.1 million years on average for a given H atom. However, in the ISM any given hydrogen atom experiences a collision with another one every 400 years, which can be calculated as follows

$$\tau_{\text{coll.}} \approx 4 \cdot 10^{11} \cdot \left(\frac{T}{\text{K}}\right)^{-1/2} \cdot \left(\frac{n_{\text{HI}}}{\text{cm}^{-3}}\right)^{-1} \quad \text{s} \tag{3.26}$$

During this collision, hydrogen atoms exchange their electrons, this being the chief mode of the hyperfine transition. If the spin orientation of the exchanged e^- changes, there will be a corresponding change in energy. Hence, collisions can result in no change, excitation, or in de-excitation. Comparing the above numbers it is clear that the relative population of the HFS levels will be governed by collisions. This eventually leads to an equilibrium stat with a ratio of aligned-to-opposed spins of 3:1, as

$$\frac{n_1}{n_0} = \frac{g_1}{g_0} \cdot e^{-\frac{h\nu_{10}}{k_B T_{\text{sp}}}} \qquad \text{and} \quad g = 2F + 1 \tag{3.27}$$

($h\nu_{10} \ll k_B T_{\text{sp}}$) T_{sp} is called "spin temperature". The energy difference corresponds to a frequency of

$$\nu_{10} = 1.420405751786(30) \text{ GHz} \tag{3.28}$$

The radiation is commonly referred to as the "21 cm emission of neutral hydrogen" or the "HI line". The fact that there is such a vast number of HI atoms along the line-of-sight means that the Hi line emission can be easily measured. The prediction that the line could be detected was made by van de Hulst in 1944 and was detected in 1951 by three groups: Euwen & Purcell, Muller & Oort and Christiansen et al..

Example: flux density of HI line within the beam of the 100 m telescope from region with $n_{\text{HI}} = 1 \text{ cm}^{-3}$ with size $L = 100$ pc which yields a column density of $N_{\text{HI}} = 3 \cdot 10^{20} \text{ cm}^{-2}$. Monochromatic power:

$$P_\nu = \frac{\dot{N} \cdot h\nu}{\nu} \cdot \Omega_{\text{mb}} \cdot D^2 \qquad D = \text{ distance} \tag{3.29}$$

$$\Omega_{\text{mb}} = 1.133 \cdot \text{HPBW}^2 = 7.8 \cdot 106{-}6 \text{ sr} \qquad \text{HPBW} = 70^\circ \cdot \frac{\lambda}{D} = 9' \tag{3.30}$$

flux density

$$S_\nu = \frac{P_\nu}{4\pi \cdot D^2} = \dot{N} \cdot h \cdot \frac{\Omega_{\text{mb}}}{4\pi} = n_{\text{HI}} \cdot L \cdot \frac{h}{4\pi} \cdot \frac{\Omega_{\text{mb}}}{\tau_{\text{coll}}} \tag{3.31}$$

photon flux

$$\dot{N} = n_{\text{HI}} \cdot \tau_{\text{coll}}^{-1} \cdot L \tag{3.32}$$

$$\Rightarrow \dot{N} = 2.4 \cdot 10^{10} \quad \text{photons cm}^{-2} \text{ s}^{-1} \tag{3.33}$$

and

$$S_\nu \approx 10^{-22} \quad \text{erg s}^{-1} \text{ cm}^{-2} \text{ Hz}^{-1} = 10 \text{ Jy} \tag{3.34}$$

...easily detectable!

3.2.2 Determination of N_{H} and T_{sp}

Because of large number of hydrogen atoms along the line-of-sight we do not know a priori whether the HI line radiation is optically thin or not. Hence, we have to go through the standard radiative transfer calculation. From Chapter ?? we have

$$\frac{dI_\nu}{ds} = \frac{1}{4\pi} \cdot n_1 \cdot A_{10} \cdot h\nu_{10} \cdot f(\nu) + \frac{I_\nu}{c} \cdot h\nu_{10} \cdot f(\nu) \cdot (B_{10} \cdot n_1 - B_{01} \cdot n_0) \tag{3.35}$$

where we identify the absorption coefficient with

$$\varkappa_\nu = -\frac{h\nu_{10}}{c} \cdot (B_{10} \cdot n_1 - B_{01} \cdot n_0) \cdot f(\nu) \tag{3.36}$$

The optical depth is

$$\tau_\nu(s) = \int_0^s \varkappa_\nu(s')ds' \tag{3.37}$$

Relate intensity I_ν to brightness temperature $T_b(\nu)$ via Rayleigh-Jeans approximation:

$$I_\nu = \frac{2k_B \cdot \nu^2}{c^2} \cdot T_\nu \tag{3.38}$$

The spin temperature is defined via the Boltzmann statistics of the population of the HFS levels:

$$\frac{n_1}{n_0} = \frac{g_1}{g_0} \cdot e^{-\frac{h\nu_{10}}{k_B T_{\mathrm{sp}}}} \approx \frac{g_1}{g_0} \cdot \left(1 - \frac{h\nu_{10}}{k_B T_{\mathrm{sp}}}\right) =: \frac{g_1}{g_0} \cdot \left(1 - \frac{T_{10}}{T_{\mathrm{sp}}}\right) \tag{3.39}$$

$$T_{10} = \frac{h\nu_{10}}{k_B} = 0.068 \text{ K} \ll T_{\mathrm{sp}} \tag{3.40}$$

We furthermore use the relations between the Einstein coefficients

$$g_0 \cdot B_{01} = g_1 \cdot B_{10} \qquad \text{and} \qquad A_{10} = \frac{8\pi \cdot h \cdot \nu_{10}^3}{c^3} \cdot B_{10} \tag{3.41}$$

With the above we derive

$$\varkappa_\nu = \frac{h\nu_{10}}{c} \cdot B_{01} \cdot n_0 \cdot \left(1 - \frac{B_{10}}{B_{01}} \cdot \frac{n_1}{n_0}\right) \cdot f(\nu) \tag{3.42}$$

$$= \frac{h\nu_{10}}{c} \cdot \frac{g_1}{g_0} \cdot B_{01} \cdot n_0 \cdot \left(1 - \frac{g_0}{g_1} \cdot \frac{n_1}{n_0}\right) \cdot f(\nu) \tag{3.43}$$

$$= \frac{3c^2 \cdot A_{10} \cdot n_0}{8\pi \cdot \nu_{10}^2} \cdot \left(1 - e^{-\frac{h\nu_{10}}{k_B T_{\mathrm{sp}}}}\right) \cdot f(\nu) \tag{3.44}$$

$$\approx \frac{3c^2 \cdot A_{10} \cdot n_0}{8\pi \cdot \nu_{10}^2} \cdot \frac{h\nu_{10}}{k_B T_{\mathrm{sp}}} \cdot f(\nu) \tag{3.45}$$

Since

$$n_{\mathrm{HI}} = n_0 + n_1 = n_0 + 3n_0 = 4n_0 \tag{3.46}$$

we finally obtain

$$\boxed{\varkappa_\nu = \frac{3 \cdot h \cdot c^2}{32\pi} \cdot \frac{A_{10}}{\nu_{10}} \cdot \frac{n_{\mathrm{HI}}}{k_B T_{\mathrm{sp}}} \cdot f(\nu)} \tag{3.47}$$

translate $f(\nu)$ to $f(v)$:

$$f(\nu)d\nu = f(v)dv \tag{3.48}$$

$$f(\nu) = f(v) \cdot \frac{dv}{d\nu} \tag{3.49}$$

$$\frac{v}{c} = \frac{\nu_{10} - \nu}{\nu_{10}} \Rightarrow \frac{dv}{d\nu} = -\left(\frac{v_{10}}{c}\right)^{-1} \tag{3.50}$$

and with

$$d\tau_\nu = d\varkappa_\nu ds \tag{3.51}$$

we have

$$d\tau(v) = 5.4728 \cdot 10^{-19} \cdot \left(\frac{n_{\mathrm{HI}}}{\mathrm{cm}^{-3}}\right) \cdot \left(\frac{T_{\mathrm{sp}}}{\mathrm{K}}\right)^{-1} \cdot \left(\frac{f(v)}{\mathrm{km}^{-1}\ \mathrm{s}}\right) \cdot \left(\frac{ds}{\mathrm{cm}}\right) \tag{3.52}$$

Integrating over all velocities (= frequencies) on the left side and over the whole line-of-sight on the right, can proceed to arrive at the total HI column density:

$$\int_{-\infty}^{+\infty} \tau(v) \left(\frac{dv}{\mathrm{km\ s}^{-1}}\right) = 5.47 \cdot 10^{-19} \cdot \left(\frac{T_{\mathrm{sp}}}{\mathrm{K}}\right)^{-1} \cdot \int_0^{s_0} \left(\frac{n_H(s)}{\mathrm{cm}^{-3}}\right) \left(\frac{ds}{\mathrm{cm}}\right) \tag{3.53}$$

or, defining the column density as

$$N_H = \int_0^{s_0} n_H(s) ds \quad \text{, or here} \quad N_H(v) \int_0^{s_0} n_H(s,v) ds \tag{3.54}$$

we derive this column densitiy by integrating the optical depth over velocity

$$\left(\frac{N_{\mathrm{HI}}}{\mathrm{cm}^{-2}}\right) = 1.823 \cdot 10^{18} \cdot \left(\frac{T_{\mathrm{sp}}}{\mathrm{K}}\right) \cdot \int_{-\infty}^{+\infty} \tau(v) \left(\frac{dv}{\mathrm{km\ s}^{-1}}\right) \tag{3.55}$$

The frequency or velocity dependence of optical depth is

$$d\tau(v) = c \cdot n_{\mathrm{HI}} \cdot T_{\mathrm{sp}}^{-1} \cdot f(v) ds \tag{3.56}$$

with $c = 5.47 \cdot 10^{-19}$ cm^2 K km s^{-1}; from radiative transfer we have

$$T_b(v) = T_{\mathrm{sp}} \cdot \left[1 - e^{-\tau(v)}\right] + T_c \cdot e^{-\tau(v)} \tag{3.57}$$

where T_c is the brightness temperature of a background source. For $\tau(v) \ll 1$ we simplify this to

$$T_b(v) = \tau(v) \cdot T_{\mathrm{sp}} \tag{3.58}$$

Then $T_b(v)$ is the brightness temperature measured in each velocity interval dv. Inserting numbers for c we find

$$\boxed{N_{\text{HI}} = 1.823 \cdot 10^{18} \cdot \int_0^\infty \left(\frac{T_b(v)}{\text{K}}\right) \cdot \left(\frac{dv}{\text{km s}^{-1}}\right) \quad \text{atoms cm}^{-2}} \tag{3.59}$$

In the most general case, the radiative transfer calculation would result in a an observed brightness temperature of

$$T_b(v) = T_{\text{bg}}(v) \cdot e^{-\tau(v)} + T_{\text{sp}} \cdot \left[1 - e^{-\tau(v)}\right] \tag{3.60}$$

where $T_{\text{bg}}(v)$ is the brightness temperature incident of the far side of an HI cloud. As we are only interested in the HI emission (and wish to get rid of the background continuum), we usually measure the difference between the two components

$$\Delta T_b(v) = T_b(v) - T_{\text{bg}} = (T_{\text{sp}} - T_{\text{bg}}) \cdot \left[1 - e^{-\tau(v)}\right] \tag{3.61}$$

This is accomplished either by on-off measurements, also called position switching, or by frequency-switching. In order to gain some physical feeling for the above equation, let us consider the two extreme cases of $\tau \ll 1$ and $\tau \gg 1$ for a single cloud and without any background radiation.

- $\tau(v) \ll 1$
  In this case, with $T_{\text{bg}} = 0$, we have

  $$T_b(v) = T_{\text{sp}} \cdot \tau(v) = c \cdot N_{\text{HI}}(v) \tag{3.62}$$

  i.e. the measured brightness temperature is proportional to the column density of HI per unit velocity. This means that essentially all of the spontaneously emitted 21 cm photons escape the cloud without being absorbed. The emission is pracically independent of T_{sp}, since $T_0 = h\nu_{10}/k_B$ is much smaller than any reasonable T_{sp}. Thus the number of photons leaving the cloud tells us directly what the HI column density is.

- $\tau(v) \gg 1$
  In this case, we have (with $T_{\text{bg}} = 0$)

  $$T_b = T_{\text{sp}} \tag{3.63}$$

  i.e. we directly measure the spin temperature. Any 21 cm photons emitted some where within the cloud are intantly absorbed by foreground HI atoms. Only photons with $\tau \lesssim 1$ emitted from the front surface (facing us) leave the cloud. Hence, the observed brightness temperature is independent of the column density and depends only on the cloud temperature (analogy to black body radiation in case of thermal continuum).

Measuring $\Delta T_b(v)$ implies that we see emission or absorption, depending on whether $T_{\text{sp}} > T_{\text{bg}}$ or $T_{\text{sp}} < T_{\text{bg}}$.

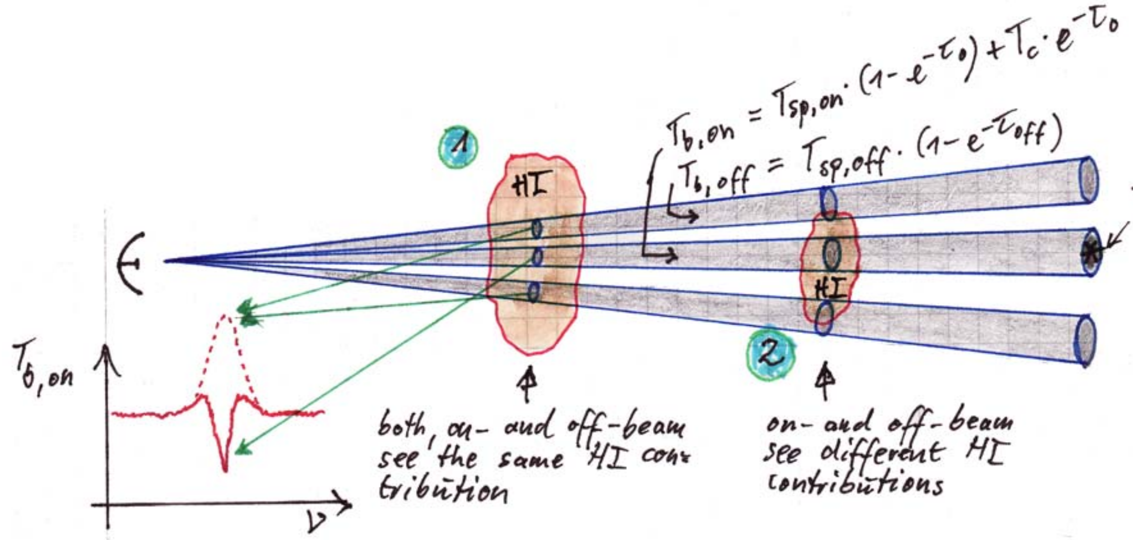

Figure 3.5: Scematic of position switching

If the 3 K CMB were the only excitation mechanism for the 21 cm line, the we would be faced with the special case $T_{\rm sp} = T_{3\,\rm K} = 2.728$ K. The neutral hydrogen would then remain ivisible except in the direction of strong radio continuum sources, where $T_{\rm bg}$ would exceed the 3 K background. Fortunatly, there are two other excitation mechanisms at work: collisions and Ly-α radiation.

$$T_{b,\rm on} = T_{\rm bg} \cdot e^{-\tau_{\rm on}} + T_{\rm sp,on} \cdot \left(1 - e^{-\tau_{\rm on}}\right) \tag{3.64}$$

With frequency switching, we measure the above and, sufficiently far off the line, we measure the pure continuum of the background source. Substracting them, we obtain

$$\Delta T_b = T_{b,\rm on} - T_{\rm bg} = (T_{\rm sp,on} - T_{\rm bg}) \cdot \left(1 - e^{-\tau_{\rm on}}\right) \tag{3.65}$$

The pure line emission can be estimated using several off-spectra that still see HI emission from the cloud:

$$T_{b.\rm HI} \approx \langle T_{b,\rm off}\rangle = \langle T_{\rm sp,off}\rangle \cdot \left(1 - e^{-\langle\tau_{\rm off}\rangle}\right) \tag{3.66}$$

Generally, we have $\langle\tau_{\rm off}\rangle \neq \tau_{\rm on}$ and $\langle T_{\rm sp,off}\rangle \neq T_{\rm sp,on}$. If, however, the two conditions are nearly fulfilled, then we can derive $T_{\rm sp}$ and/or $\tau_{\rm on}$.

- $\langle T_{\rm sp,off}\rangle = T_{b,\rm HI}$
  This is nearly fulfilled if the antenna beam is small compared to the angular dimension of the HI cloud (denoted 1 in the figure). Then, from equation 3.65 it follows that

$$\frac{\langle T_{\rm sp,off}\rangle - \Delta T_b}{T_{\rm bg}} = \frac{T_{b,\rm HI} - \Delta T_b}{T_{\rm bg}} \tag{3.67}$$

$$= \frac{T_{\rm sp,off} \cdot \left(1 - e^{-\tau_{\rm on}}\right) - (T_{\rm sp,on} - T_{\rm bg}) \cdot \left(1 - e^{-\tau_{\rm on}}\right)}{T_{\rm bg}} \tag{3.68}$$

$$= 1 - e^{-\tau_{\rm on}} \tag{3.69}$$

If $\tau_{\rm on} \ll 1$

$$\tau_{\rm on} = \frac{\langle T_{\rm sp,off}\rangle - \Delta T_b}{T_{\rm bg}} \tag{3.70}$$

otherwise

$$\boxed{\tau_{\rm on} = -\ln\left(1 - \frac{T_{b,\rm HI} - \Delta T_b}{T_{\rm bg}}\right)} \tag{3.71}$$

- $\langle T_{\rm sp,off}\rangle = T_{\rm sp,on}$, $\langle \tau_{\rm off}\rangle = \tau_{\rm on}$

We have seen that

$$\varkappa_\nu \propto T_{\rm sp}^{-1} \quad \text{,i.e. } \tau_\nu \propto T_{\rm sp}^{-1} \tag{3.72}$$

and

$$\Delta T_b(v) = (T_{\rm sp} - T_{\rm bg}) \cdot \left[1 - e^{-\tau(v)}\right] \tag{3.73}$$

That means, if $T_{\rm sp}$ is large we have emission and if $T_{\rm sp}$ is small we have absorption, i.e. cold gas clouds are seen in absorption and warm (hot) gas is seen in emission.

Observations indicate that $T_{\rm sp}$ is in between 10 K and 5000 K, and the number density $n_{\rm HI}$ is between 0.2 cm^{-3} and 10 cm^{-3}. With pressure balance holding, i.e.

$$P_1 = n_1 \cdot k_B \cdot T_1 = P_2 = n_2 \cdot k_B \cdot T_2 \tag{3.74}$$

e.g. $n_1 = 10$ cm^{-3}, $n_2 = 0.2$ cm^{-3}, $T_1 = 50$ K, $T_2 = 2500$ K

Frames of reference for v:

heliocentric corrects for earth rotation and motion about the sun $\rightarrow \quad v_{\rm rel}$

local standard of rest corrects in addition for peculiar motion of the sun with respect to surrounding nearby stars, as measured from their proper motions; the sun moves at 20 km s^{-1} towards $\alpha_{1900} = 18^{\rm h}$, $\delta_{1900} = 30^\circ \;\Rightarrow\; v_{\rm LSR}$

3.3 Constituents of the diffuse ISM

Gas, dust, relativistic plasma; for the gas we know 5 components (see Wolfire et al., 1996, Ap. J. 443, 152)

	MM	CNM	WNM	WIM	HIM
n [cm^{-3}]	$10^2 \cdots 10^5$	$4 \cdots 80$	$0.1 \cdots 0.6$	$\simeq 0.2$	$10^{-3} \cdots 10^{-2}$
T [K]	$10 \cdots 50$	$50 \cdots 200$	$5500 \cdots 8500$	$\simeq 8000$	$10^5 \cdots 10^7$
h [pc]	$\simeq 70$	$\simeq 140$	$\simeq 400$	$\simeq 900$	$\geqq 1000$
$f_{\rm vol}$	$< 1\%$	$\simeq 2 \cdots 4\%$	$\simeq 30\%$	$\simeq 20\%$	$\simeq 50\%$
$f_{\rm mass}$	$\simeq 20\%$	$\simeq 40\%$	$\simeq 30\%$	$\simeq 10\%$	$\simeq 1\%$

MM molecular medium

CNM cold neutral medium

WNM warm neutral medium

WIM warm ionized medium

HiM hot ionized medium

CNM resident in relatively dense clouds, occupying a significant fraction of the interstellar volume. High density implies high cooling rates $\Rightarrow$ a lot of energy is needed to keep the temperature: $L \approx 10^{42}$ erg s^{-1}. Produces narrow ($\langle\sigma_v\rangle \approx 1.7$ km s^{-1}) features in emission spectrum, which can be readily identified as narrow ones in absorption[1]; termed "HI clouds"; they turn out, however, to be filamentary and sheet-like, rather than spherical; don't show up on every line-of-sight, in contrast to WNM

WNM roughly 30% of total HI; low volume density, but non-negligible filling factor; low density $\Rightarrow$ low cooling rates, so total power required to heat is comperatively small; distribution derived from HI emission; Mebold (1972) decomposed $\simeq 1200$ spectra into narrow ($\sigma_v \lesssim 5$ km s^{-1}) and broad (5 km s^{-1} $< \sigma_v <$ 17 km s^{-1}) gaussian components, showing ominpresence of broad components.

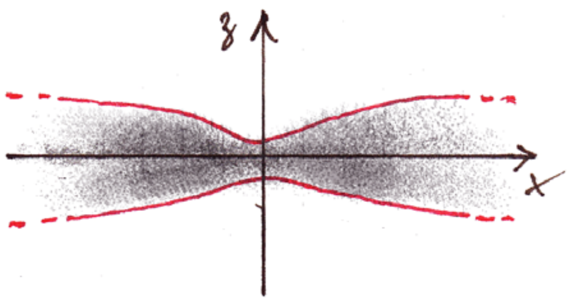

Neutral hydrogen distributed in a flaring disk, according to the gravitational potential. The scale heights for the CNM and WNM are $h_{\rm CNM} \approx 140$ pc and $h_{\rm WNM} \approx 400$ pc. Radial distribution frequently exhibits a central depression, reaches maximum at about $8 \cdots 10$ kpc, beyond which it declines below the (current) detection threshold, i.e. $N_{\rm HI} \lesssim 10^{19}$ cm^{-2}.

N.B.: at column densities $\lesssim 10^{21}$ cm^{-2} star formation is strongly suppressed (shielding against UV radiation that dissociates molecules; Jeans instabilities).

Kinematically, one distinguishes between:

- low-velocity gas, LVCs = low-velocity clouds
- intermediate-velocity gas, IVCs = intermediate-velocity clouds
- high-velocity gas, HVCs = high velocity clouds

LVCs follow normal galactic rotation and are located within the gaseous disk

[1] Since $\tau \propto T_{\rm sp}^{-1}$

IVCs have velocities between LVCs and HVCs (see below), with metallicities close, $|z| \lesssim 1$ kpc.

HVCs have $|\Delta v| = |v_{\rm HVC} - v_{\rm rot}| > 50$ km s^{-1}; more distant than IVCs, but few reliable distance determinations only; e.g.
"complex A": $D = 2.5 \cdots 7$ kpc $\rightarrow M_{\rm HI} = 10^5 \cdots 2 \cdot 10^6$ M$_\odot$
"Magellanic Stream": $M_{\rm HI} \approx 10^8$ M$_\odot$(for $D = 50$ kpc)

Origin: LVCs disk clouds; IVCs galactic fountains "raining back" onto disk; LVCs ?? former fountains ? but low metals or: tidal debris from infalling [ler. gals.], gas from outer disk

Data cubes. Mapping HI line with a radio telescope results in so-called data cube, with brightness temperature $T_b = T_b(\xi, \eta, v)$. The arrangement is usually such that a map of T_b is computed for each velocity channel. From this, the so-called moment maps are calculated:

$$N_{\rm HI}(\xi, \eta) = C \cdot \int T_b(\xi, \eta)\, dv \qquad \text{moment 0 or column density} \tag{3.75}$$

$$\langle v(\xi, \eta)\rangle = \frac{\int T_b(\xi, \eta)\, v(\xi, \eta)\, dv}{\int T_b(\xi, \eta)\, dv} \qquad \text{moment 1 or velocity field} \tag{3.76}$$

$$\langle \sigma(\xi, \eta)\rangle = \frac{\int T_b(\xi, \eta)\, v^2(\xi, \eta)\, dv}{\int T_b(\xi, \eta)\, dv} \qquad \text{moment 2 or velocity dispersion} \tag{3.77}$$

HI in galaxies. ellipticals generally lack neutral gas; dwarf irregular and spiral galaxies invariably possess disks of neutral gas; relative amount of HI

$$\frac{M_{\rm HI}}{M_{\rm rot}} = \underbrace{3\%}_{\text{massive spirals}} \cdots \underbrace{20\%}_{\text{gas-rich dwarfs}} \qquad \text{but mostly dark matter!} \tag{3.78}$$

3.4 Examples

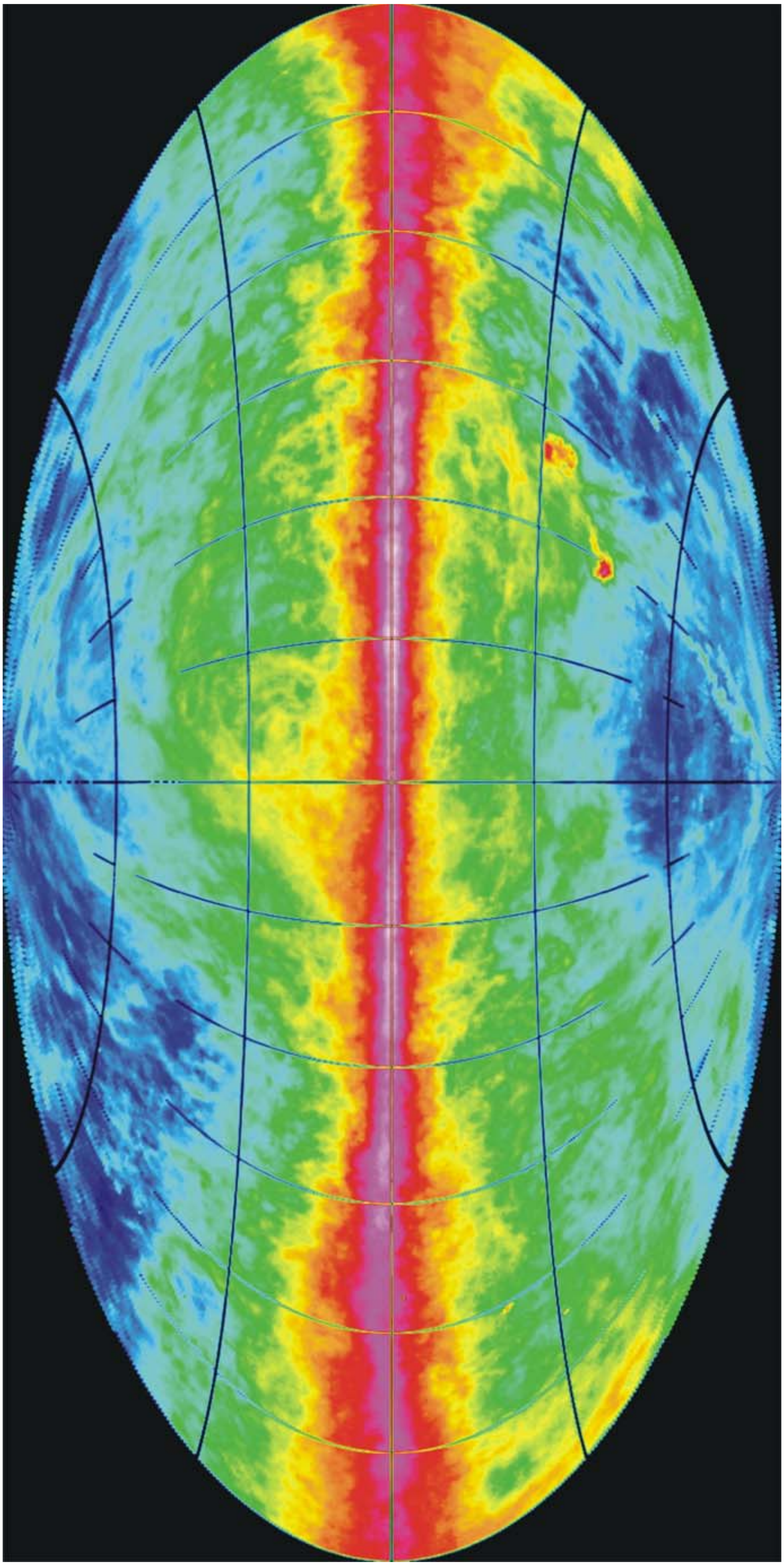

Figure 3.6: The Milky Way in neutral hydrogen

Figure 3.7: NGC6946 in the optical and neutral hydrogen

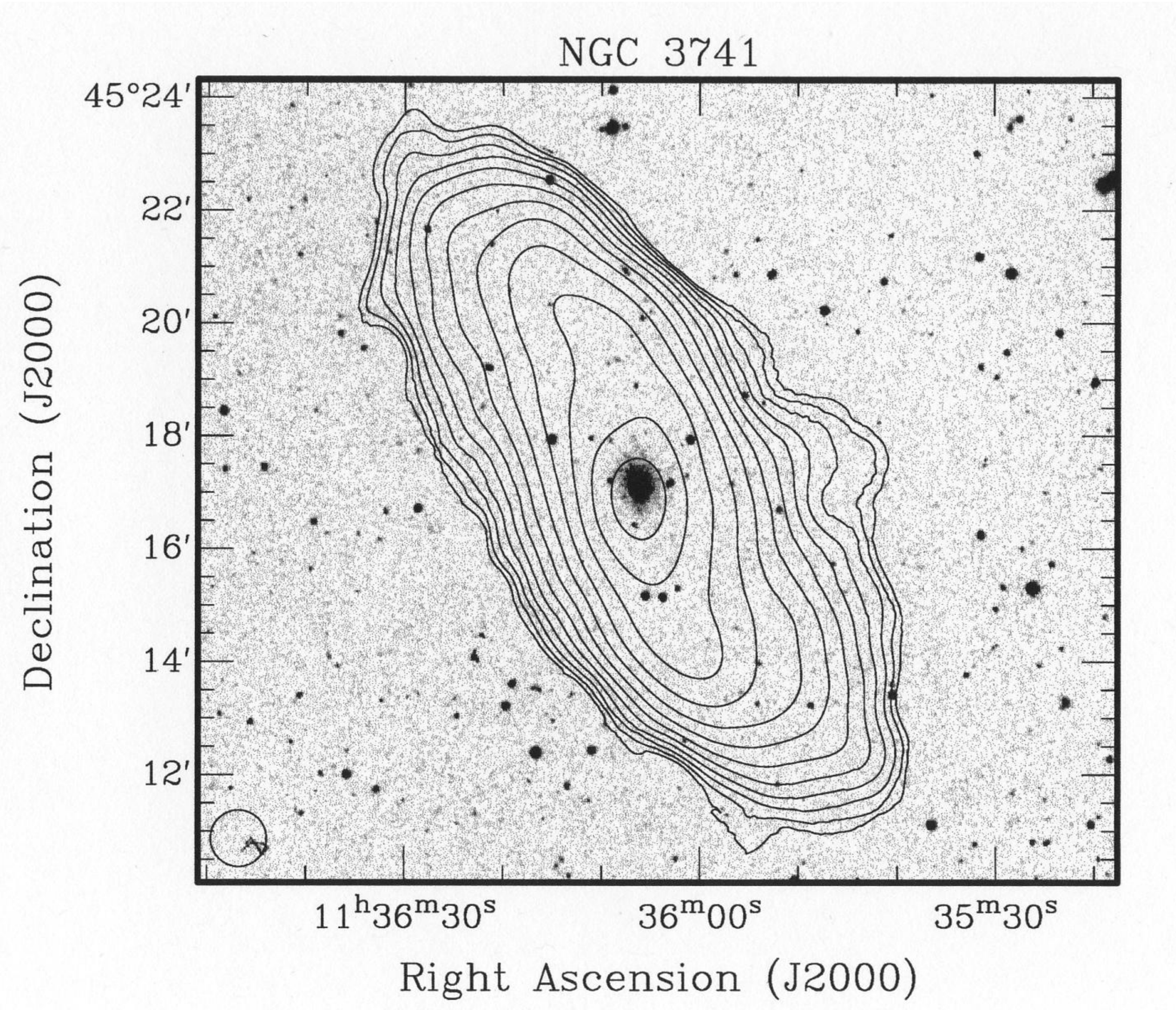

Figure 3.8: NGC3741 in the optical with a neutral hydrogen map superimposed